



Suitability of RPMI 2650 cell models for nasal drug permeability prediction

Nadica Sibinovska^a, Simon Žakelj^a, Katja Kristan^{b,c,*}

^a University of Ljubljana, Faculty of Pharmacy, Chair of Biopharmaceutics and Pharmacokinetics, Aškerčeva c. 7, SI- 1000 Ljubljana, Slovenia

^b Institute of Biochemistry, Faculty of Medicine, University of Ljubljana, Vrazov trg 2, 1000 Ljubljana, Slovenia

^c Lek Pharmaceuticals, d.d., Sandoz Development Center Slovenia, Verovškova 57, 1526 Ljubljana, Slovenia



ARTICLE INFO

Keywords:

RPMI 2650
Air–liquid interface
Liquid–liquid interface
Drug permeability
Nasal drug absorption
Permeability method suitability

ABSTRACT

The RPMI 2650 cell line has been a subject of evaluation as a physiological and pharmacological model of the nasal epithelial barrier. However, its suitability for drug permeability assays has not yet been established on a sufficiently large set of model drugs. We investigated two RPMI 2650 cell models (air-liquid and liquid-liquid) for nasal drug permeability determination by adopting the most recent regulatory guidelines on showing suitability of *in vitro* permeability methods for drug permeability classification. The permeability of 23 model drugs and several zero permeability markers across the cell models was assessed. The functional expression of two efflux transporters P-glycoprotein (P-gp) and Breast Cancer Resistant Protein (BCRP) was shown to be negligible by bidirectional transport studies using appropriate transporter substrates and inhibitors. The model drug permeability determined in the two RPMI 2650 cell models was correlated with the fully differentiated nasal epithelial model (MucilAir™). Additionally, correlations between the drug permeability in the investigated cell models and the ones determined in the Caco-2 cells and isolated rat jejunum were established. In conclusion, the air-liquid RPMI 2650 cell model is a promising pharmacological model of the nasal epithelial barrier and is much more suitable than the liquid-liquid model for nasal drug permeability prediction.

1. Introduction

In addition to the nasal mucosa being an important target for local drug delivery during the treatment of upper respiratory diseases such as rhinitis or congestion, it is also recognized as an alternative route for non-invasive systemic drug administration, due to its characteristics [1–5]. Namely, its substantial vascularization and high permeability, along with the circumvention of pre-systemic metabolism enable rapid drug absorption [2,3,6]. The number of intranasally administered active substances having systemic effect which emerged on the market has increased (drugs for severe pain relief, anti-migraine drugs), while more efforts are being made to develop adequate drug formulations [1,5].

The screening of intranasal drug candidates and drug formulations requires the use of suitable and reliable models of the nasal barrier which would allow conduction of permeability assays with an aim to predict drug absorption and bioavailability [5–7]. Although excised nasal tissue is the closest match to the nasal mucosa in terms of histology, cell type distribution and expression of drug transporters, the poor availability and high heterogeneity make it unsuitable for high-throughput screening [5,8]. Also, the use of excised animal tissues can raise ethical concerns and introduces the issue of interspecies

variability [6,8,9]. The primary human nasal epithelial cells are morphologically and biochemically the nearest possible equivalent to the excised tissue [8]. Nevertheless, the high transepithelial electrical resistance (TEER) value maintained $> 500 \Omega\text{cm}^2$ during 2 weeks of culturing [10] is considerably greater than the reported TEER values of excised human ($40\text{--}120 \Omega\text{cm}^2$) or animal ($90\text{--}180 \Omega\text{cm}^2$) nasal mucosa [11], which might affect the suitability of primary human nasal epithelial cells as a physiologically relevant nasal barrier model in some aspects [9]. Genetic stability and higher reproducibility can be achieved when immortalized cell lines are used as nasal barrier models, providing a source for extensive cell proliferation [5].

The only immortalized cell line of human origin that has gained a reawakened research interest in the past decade is the RPMI 2650 cell line [8]. It originates from an anaplastic squamous cell carcinoma of the human nasal septum and does not show alteration of the normal diploid karyotype, as it maintains high stability throughout continuous *in vitro* culturing [12,13]. Since the first finding that the air-liquid (A-L) culturing interface is crucial for appropriate differentiation of the RPMI 2650 cells [14], several research groups attempted to characterize this human nasal epithelial cell line and optimize it as a suitable *in vitro* model of the nasal barrier [5,11,15–17]. This cell line demonstrates resemblance to the normal human nasal epithelium in terms of

* Corresponding author at: Lek Pharmaceuticals, d.d., Sandoz Development Center Slovenia, Verovškova 57, 1526 Ljubljana, Slovenia.

E-mail address: katja.kristan@sandoz.com (K. Kristan).

<https://doi.org/10.1016/j.ejpb.2019.10.008>

Received 22 July 2019; Received in revised form 1 October 2019; Accepted 18 October 2019

Available online 19 October 2019

0939-6411/ © 2019 Elsevier B.V. All rights reserved.

production of mucus material at the cell surface and nasal barrier integrity, reaching TEER values similar to those of the excised human and animal nasal tissues [5,15,16]. It expresses a variety of cell junction proteins, including ZO-1, occludin, claudin-1, E-cadherin, and β -catenin [11,14,16], while the expression of drug transporters in this cell line has recently been brought into focus with some of the functional characterization still pending [9,11,15,18,19].

Whenever an *in vitro* cell model is intended to be used as a screening tool for drug absorption, as well as to evaluate the function of drug transporters, it is essential to confirm its suitability and reliability as appropriate physiological and pharmacological epithelial barrier model. Moreover, it is necessary to use a large enough set of properly selected model drugs to determine the model predictiveness [20].

Permeability assays which utilize Caco-2 cell monolayers are widely used to estimate intestinal drug absorption in humans. However, the employment of the Caco-2 assays in support of high permeability for Biopharmaceutical Classification System (BCS) classification is limited to passively transported drugs. The new U.S. Food and Drug Administration (FDA) guidance from December 2017 [21] and the draft version of the ICH harmonized guideline from June 2018 [22] on demonstration of suitability of the *in vitro* permeability methods for permeability classification recommend the use of at least 20 model drugs covering the full permeability range (low, moderate and high permeability category), while confirming the cell layer integrity throughout the permeability assays. Moreover, in both guidelines, the bidirectional transport studies using adequate transporter substrates at non-saturating concentrations are mentioned as means to demonstrate functional expression of efflux transporters [21,22]. Once the suitability of the *in vitro* permeability method is established, internal standards should be chosen in order to show method consistency when drug transport studies are employed in permeability determination for new drug candidates. Acceptance criteria for the internal standards can be also set [22].

The objective of our study is to evaluate the suitability of the air-liquid (A-L) and liquid-liquid (L-L) cultured RPMI 2650 cell layers as pharmacological nasal barrier model for drug permeation studies. This is achieved by correlating the permeability for a set of 23 differently classified model drugs with literature data on two well established intestinal permeability models, as well as with published and our data on the commercially available organotypic 3D model of the nasal mucosa (MucilAir™).

2. Materials and methods

2.1. Materials

Advanced Minimum Essential medium (A-MEM), heat inactivated fetal bovine serum (FBS), GlutaMAX™ Supplement, Hank's balanced salt solution (HBSS), 4-(2-hydroxyethyl)piperazine-1-ethanesulfonic acid (HEPES), TrypLE™ Select were purchased from Thermo Fisher Scientific (Waltham, MA, USA). Tissue culture flasks were obtained from Sarstedt (Nümbrecht, Germany), while Millicell® 24-well cell culture plate assemblies (consisting of 24-well cell culture plate, single-well feeder tray and lid) and 24-well receiver trays were purchased from Merck Millipore (Tullagreen, Ireland). Model drug substances and chemicals were obtained from Sigma-Aldrich (Munich, Germany). PSC-833 and Ko143 were obtained from Solvo Biotechnology (Budapest, Hungary) and Tocris Bioscience (Bristol, UK), respectively. All solutions were prepared in HBSS buffer with 0.01 M HEPES (assay buffer). When the desired concentrations could not be achieved due to low solubility of the compounds, assay buffer with 1% DMSO (Sigma-Aldrich (Munich, Germany)) was used.

2.2. Cell cultures

2.2.1. RPMI 2650 cells

RPMI 2650 cells were obtained from the European Collection of Cell Cultures, Health Protection Agency (Cat.No. 88031602, Lot No. 10D028, passage number 10, STR verification: 08.06.2010, PCR based mycoplasma detection: 11.06.2010) and used between passages 29–41 for permeability assays. The RPMI 2650 cells were cultured in polystyrene tissue culture flasks at 37 °C, 5% CO₂ and 95% relative humidity in A-MEM supplemented with 2% GlutaMAX™ and 2.5% FBS. The cell culture medium was changed three times per week. After reaching 80–90% confluence in the culture flasks, RPMI 2650 cells were detached by treatment with TrypLE™ Select and seeded at a density of 2×10^5 cells/cm² on polyethylene terephthalate (PET) membranes (1 μ m pores, 0.7 cm²) in Millicell® 24-well cell culture plates. In order to establish L-L interface, adequate volumes of cell culture medium were added to the apical (400 μ L medium/insert) and basolateral compartments (22–24 mL medium/feeder tray), while for the A-L interface, the medium from the apical compartment was removed 3 days post-seeding. The cell culture medium was changed every 2–3 days. The cells were used for permeability assays after three weeks of culturing.

2.2.2. 3D human nasal epithelial cell culture- MucilAir™

MucilAir™ cultures were received from Epithelix Sarl (MucilAir pool of 14 donors, cell type hAEC/Nasal, Product code: EP02, Batch number: MP0008, Geneva, Switzerland) as differentiated epithelia grown on 24-well culture Transwell inserts with 0.4 μ m pore size and 6.5 mm diameter (Costar 3470, Corning Incorporated, New York, NY, USA). The cell culture was maintained under A-L interface in humidified atmosphere at 37 °C and 5% CO₂, according to the supplied provider's growth protocol. The 700 μ L of a commercially available chemically defined serum-free culture medium (Epithelix Sarl, Geneva, Switzerland) was added only to the basolateral side of cells, with medium change at every 2–3 days.

2.3. Permeability assays using RPMI 2650 cells

2.3.1. Permeability of model drugs and zero permeability markers

RPMI 2650 cells were cultured at A-L and L-L interface, as previously described. Prior to conducting the permeability assay, the RPMI 2650 cells were rinsed twice with assay buffer, pre-warmed at 37 °C, followed by TEER measurement performed with a tissue resistance measuring system with REMS autosampler (World Precision Instruments, Sarasota, USA). The measured TEER values were corrected by subtracting the resistance of blank porous membranes, while also considering the porous membrane surface area.

The tested model drug substances and zero permeability markers, as well as the used concentrations are shown in Table 1. The permeability of the model drugs and zero permeability markers was assessed in both directions: apical to basolateral (A-B) and basolateral to apical (B-A). For the transport studies in A-B direction, 400 μ L of pre-warmed test solutions were added in the apical compartment, while 800 μ L of pre-warmed assay buffer were added to the basolateral side. When assessing permeability in B-A direction, 400 μ L of pre-warmed assay buffer and 800 μ L of pre-warmed test solutions were added to the apical and basolateral compartments, respectively. The 24-well cell culture plates with RPMI 2650 cells were incubated at 37 °C in a humidified 5%CO₂/95% air atmosphere throughout the experiment. The 100 μ L samples were withdrawn from the acceptor wells (150 μ L only for azilsartan and rosuvastatin) at predetermined time points (30, 60, 90, 120 and 180 min), whereas 20 or 10 μ L samples were withdrawn from the donor wells for the model drugs or zero permeability markers, respectively, at 0 and 180 min. The volume withdrawn was replaced with fresh assay buffer or donor solution. Following sample collection, the RPMI multilayers were gently washed with assay buffer and the TEER was measured as described before. In order to evaluate the RPMI 2650 cell

Table 1

Summary of doses used for testing permeability of investigated compounds and zero permeability markers (ZPM), dissolved in 250 mL assay buffer and data on permeability category.

Tested substance	Tested concentration (mg/250 mL)	Permeability category based on oral absorbed fraction (f_a)	f_a (%) [23] ^g
Theophylline	60	high	100
Propranolol ^b	80	high	100
Verapamil ^b	75	high	100
Antipyrine	50	high	99
Carbamazepine ^a	10	high	98
Rosiglitazone ^a	4	high	97
Ketoprofen ^a	100	high	95
Ropinirole ^b	500	high	90
Metoprolol ^c	100	high	95
Losartan ^d	50	moderate	65
Furosemide ^a	80	moderate	61
Amiloride ^b	5	moderate	60
Hydrochlorothiazide ^a	50	moderate	55
Ranitidine ^b	300	moderate	50
Atenolol	100	moderate	50
Rosuvastatin ^{a, c}	13	moderate	50
Famotidine ^a	40	low	45
Oxacillin ^f	500	low	33
Nadolol	64	low	27
Acyclovir ^a	11	low	23
Chlorothiazide ^a	4 (A-L model); 8 (L-L model)	low	20
Enalaprilat	18	low	10
Azilsartan ^a	19	low [24]	No data available
FD 3–5 kDa	50	ZPM	
FD 10 kDa	50	ZPM	
FD 20 kDa	50	ZPM	
FD 40 kDa	50	ZPM	
FD 70 kDa	50	ZPM	

^a DMSO used for preparing solutions of model drugs (maximum 1% DMSO in the final solution).

^b Tested substances used in their hydrochloride salt form.

^c Substance tested as metoprolol tartrate.

^d Substance tested as losartan potassium.

^e Substance tested as rosuvastatin calcium.

^f Substance tested as oxacillin sodium monohydrate.

^g Ref. [23] used for f_a (%) of all tested compounds, except for ropinirole [25] and rosuvastatin [26].

integrity, the cells were subsequently incubated with 20 μ M Lucifer Yellow (LY) solution for 1 h under standard incubating conditions. After 60 min incubation period, 100 μ L samples were withdrawn from the acceptor wells and their fluorescence was measured using microtiter plate reader (Infinite M1000, Tecan, Switzerland).

2.3.2. ABC transporter functionality studies

The functional activity of P-gp and BCRP transporters was investigated by performing bidirectional transport studies according to the ICH [22] and FDA [21] guidelines, using appropriate model transporter substrates and selective inhibitors. Namely, rhodamine123 (20 μ M) was used as a P-gp substrate, while verapamil (200 μ M) and PSC-833 (10 μ M) were used as inhibitors in both RPMI 2650 cell models for combined P-gp – BCRP and selective P-gp inhibition, respectively. When investigating the functional activity of BCRP, rosuvastatin (50 μ M) and chlorothiazide (50 μ M) were used as model BCRP substrates and Ko143 (5 μ M) as a selective inhibitor.

The transporter functionality was tested by performing bidirectional transport studies, using donor solutions of the substrate only, as well as using donor solutions that contain both the substrate and the inhibitor. The bidirectional transport study protocol was performed as described in section 2.3.1 (Permeability of model drugs and zero permeability markers).

2.4. Permeability assays using MucilAir™

Before the permeability assay, apical washing for the inserts with MucilAir™ was done with assay buffer, pre-warmed at 37 °C, followed by TEER measurement performed with an EVOM (epithelial tissue volt-ohmmeter) and STX2 electrodes (World Precision Instruments, Sarasota, USA). The following model drugs were tested: furosemide, famotidine, losartan, azilsartan and oxacillin. The tested concentrations are shown in Table 1. The permeability of the model drugs was assessed in A-B direction for all drugs in triplicates, while the permeability in B-A direction was also tested for furosemide and losartan. For the transport studies in A-B direction, 250 μ L of pre-warmed test solutions were added in the apical compartment, while 700 μ L of pre-warmed assay buffer were added to the basolateral side (vice versa for B-A direction). The inserts were incubated at 37 °C in a humidified 5%CO₂/95% air atmosphere throughout the experiment. A sample volume of 100 or 150 μ L was withdrawn from the acceptor and donor wells at pre-determined time points (acceptor wells: 30, 60, 90, 120, 180 and 240 min; donor wells: 0 and 240 min) and replaced with the same volume of pre-warmed assay buffer or donor solution. The MucilAir™ epithelial cells were gently washed with assay buffer after the permeability experiment and the TEER was measured as previously described.

2.5. Analytical methods

Ultra-high pressure liquid chromatography (UHPLC Acquity separations module equipped with photodiode array detector, Empower software) (Waters, Milford, MA, USA) was used to quantify the amount of compounds which permeated through the RPMI 2650 cells and MucilAir™ epithelia, with the exception of azilsartan and rosuvastatin whose quantification was done by using high pressure liquid chromatography (Waters®e2695 HPLC separations module equipped with photodiode array detector, Empower software) (Waters, Milford, MA, USA). UHPLC and HPLC parameters for all tested model drugs are described in the work by Jarc et al. [23], except for azilsartan and rosuvastatin. The analytical method used for quantification of ropinirole is the same as the method for determination of atenolol, described in the work by Jarc et al. [23]. Quantification of rosuvastatin and azilsartan was made using Chromolith SpeedROD RP18e 50 \times 4.6 mm at 35 °C and XBridge Shield RP18 (75 \times 4.6 mm, 2.5 μ m particles) columns at 30 °C, respectively. Isocratic method with mobile phase (0.2% glacial acetic acid:ACN:THF = 70:15:15 (V:V:V)) flow of 2.0 mL/min was used for rosuvastatin. For azilsartan, mobile phase A (water:ACN:TEA = 650:350:5(V:V:V)) and mobile phase B (water:ACN:TEA = 500:500:5 (V:V:V)) were used at ratio 30:70 (V:V) at flow rate of 1.3 mL/min. The injected sample volume for rosuvastatin and azilsartan was 50 μ L, while the absorbance was detected at 248 nm and 238 nm, respectively. The amount of rhodamine123, FITC-dextran (FDs) with molecular weight (MW) 3–5 kDa, 10 kDa, 20 kDa, 40 kDa and 70 kDa and LY were quantified by measuring the fluorescence intensity at the appropriate excitation and emission wavelengths (Rhodamine 123: $\lambda_{ex/em}$ = 480/540 nm; FDs: $\lambda_{ex/em}$ = 495/515 nm and LY $\lambda_{ex/em}$ = 430/540 nm). The amount of diffused fluorescent compounds was calculated from a calibration curve.

2.6. Permeability data analysis

The apparent permeability coefficients (P_{app} s) were calculated using the Eq. (1):

$$P_{app} = k_d \times \frac{1}{A \times C_0} \quad (1)$$

where k_d (mol/s or mg/s) is the slope of the linear section in the amount or mass of investigated drug substance permeated to the acceptor side versus time plot, A is the exposed surface area of the cell monolayer (0.7 cm²), C_0 (M or mg/mL) is the average initial concentration of drug

substance in donor wells.

Calculation of efflux ratio (ER) was performed according to the Eq. (2):

$$ER = \frac{P_{app\ B-A}}{P_{app\ A-B}} \quad (2)$$

where $P_{app\ B-A}$ is the apparent permeability coefficient of drug substance in B-A direction and $P_{app\ A-B}$ is the apparent permeability coefficient of the same drug substance in A-B direction.

2.7. Statistical analysis

The statistical analysis was done using GraphPadPrism version 8.1.2 for Windows (GraphPad Software, San Diego, CA, USA). The calculated P_{app} values for the tested model drugs and zero permeability markers are expressed as mean \pm standard deviation (SD) of at least three or two replicates, respectively. Student's t-test was performed on the obtained P_{app} values of ABC transporter substrates with and without the presence of appropriate inhibitors, with the p -value < 0.05 being considered as statistically significant. The Pearson correlation coefficient (r) was calculated for the correlations between the P_{app} values obtained in RPMI 2650 cell models and in other cell or tissue models.

3. Results and discussion

Culturing RPMI 2650 cells in aseptic working area and maintaining the cell culture under controlled conditions by following an established protocol is indispensable for reaching cell confluence and proper cell differentiation throughout cultivation. As one part of the demonstration of suitability of the two RPMI 2650 cell *in vitro* models for drug permeability studies, we evaluated the models by the following criteria: multilayered epithelium integrity and functional activity of efflux transporters, while the growth of the cells in multilayer and gene expression of efflux drug transporters have been evaluated previously [11].

3.1. Barrier integrity of the RPMI 2650 A-L and L-L models

To confirm the integrity of the cell multilayers in both RPMI 2650 cell models, the TEER was measured prior to the permeability assay. Only multilayered RPMI 2650 epithelia with TEER values $> 34\ \Omega\text{cm}^2$ and $> 20\ \Omega\text{cm}^2$ for the A-L and L-L interface, respectively, measured on the day of the experiment were considered suitable to be utilized in the bidirectional transport studies, based partly on similar TEER values for the two RPMI cell models grown under the same cell culture conditions, as previously reported in a study by Kreft et al. [11] and also on the experience gained during our work.

Besides measuring the TEER of the cell multilayers, zero permeability paracellular marker compounds can be also used to confirm the epithelium integrity for drug transport [21,22,27]. P_{app} values for five FDs having different MW (3–5 kDa, 10 kDa, 20 kDa, 40 kDa and 70 kDa) were determined in both A-L (Fig. 1A) and L-L (Fig. 1B) cell models, with P_{app} values for all tested dextrans being higher for RPMI 2650 model cultured at L-L interface.

As expected, in both cell models, FD 3–5 kDa has the highest P_{app} value among the tested zero permeability markers. As shown in Fig. 1A, the same rank order for the P_{app} values of the FD with MW of 20 kDa, 40 kDa and 70 kDa determined in the RPMI 2650 A-L model was obtained, with the P_{app} values fitting in the narrow range between 3.8 and $7.0 \times 10^{-7}\ \text{cm/s}$. Unlike in the A-L model, FD 70 kDa is the only zero permeability marker that has P_{app} value $< 1.0 \times 10^{-6}\ \text{cm/s}$ in the L-L cell model. This confirms that the L-L cell model is leakier than the A-L RPMI 2650 cell model. The greater leakiness of the L-L cell model is supported by the lower TEER values of cell multilayers grown at L-L interface, as well as by lower dextran and jacalin permeability shown in

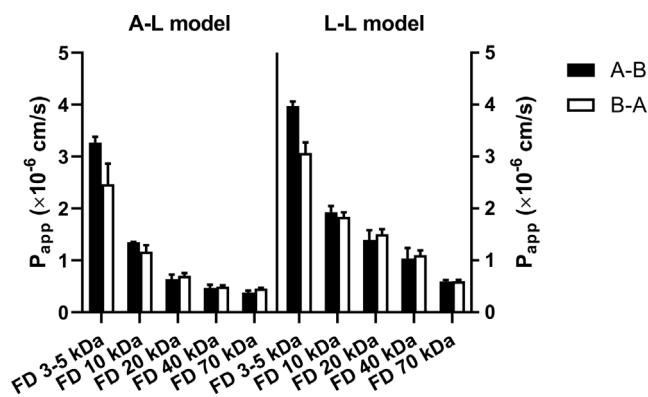


Fig. 1. Average apparent permeability coefficients (P_{app} s) of zero permeability paracellular markers FITC-dextrans (FDs) with different MW, determined in the A-L (left part of the graph) and L-L (right part of the graph) RPMI 2650 cell model. Data are expressed as the mean \pm SD. SD, standard deviation.

our previous study [11]. Moreover, higher number of cell layers is formed at A-L interface [11].

The obtained P_{app} of FD 3–5 kDa in the A-L model in our study ($3.3 \pm 0.1 \times 10^{-6}\ \text{cm/s}$) is greatly comparable to the P_{app} of 4.4 kDa FD ($2.5 \times 10^{-6}\ \text{cm/s}$) obtained in a recent study by Mercier et al. [19]. Previous permeability studies reported P_{app} of FD 4 kDa to be $0.69 \pm 0.04 \times 10^{-6}\ \text{cm/s}$ [17], which is almost 5-fold lower than the P_{app} obtained in our study. This difference is also reflected through higher reported TEER values (90–105 Ωcm^2 before the permeability assays) [17], however different culturing conditions were used (cell culture medium, pore size of filter inserts). Although the RPMI cell multilayers, like other cell models are also subject of some inter-laboratory variability, the tested markers are still properly classified with very low permeability. In other study by Kubo et al. [28], the P_{app} s for several dextrans obtained using excised rabbit nasal mucosa were very similar to the values obtained in our A-L model: $1.3 \times 10^{-6}\ \text{cm/s}$ (MW 4.4 kDa), $0.68 \times 10^{-6}\ \text{cm/s}$ (MW 9.4 kDa), $0.18 \times 10^{-6}\ \text{cm/s}$ (MW 35.6 kDa) and $0.13 \times 10^{-6}\ \text{cm/s}$ (MW 71.2 kDa). For RPMI 2650 L-L cell model, Kürti et al. [16] obtained P_{app} value of FD 4.4 kDa of $9.7 \pm 0.5 \times 10^{-6}\ \text{cm/s}$, but again cultured on different, collagen-coated inserts.

3.2. Integrity of RPMI 2650 cell multilayer during the permeability assay

Maintaining cell multilayer integrity throughout the permeability assays is essential for obtaining reliable results. The paracellular permeability of hydrophilic marker compounds (e.g. mannitol, sodium fluorescein) or high molecular weight substances such as FDs can be used as an indicator of intact cell barriers [27]. We have chosen another paracellular marker compound LY, which is transported only through tight junctions [29] to be used for assessment of multilayer integrity. Besides using LY, TEER measurement was conducted at the end of the drug permeability experiments, as it is widely accepted as suitable means of determining the integrity of tight junctions in cell culture models [27]. We incubated RPMI 2650 cell multilayers for 1 h with $20\ \mu\text{M}$ LY solution immediately after measuring TEER values at the end of the permeability assays. Only multilayered epithelia having P_{app} for LY $\leq 7 \times 10^{-6}\ \text{cm/s}$ and $\leq 11 \times 10^{-6}\ \text{cm/s}$ or alternatively having TEER values $> 25\ \Omega\text{cm}^2$ and $> 17\ \Omega\text{cm}^2$ for A-L and L-L model, respectively, at the end of the permeability assays for the model drugs, were used for establishing the suitability of the two nasal epithelial models. The set criteria for P_{app} for LY is based on our results of conducted permeability assays with this paracellular marker compound, while the TEER values at the end of the permeability assays indicating sufficient barrier integrity, represent a 25% decrease of the acceptable TEER values measured prior to the permeability studies, as stated in

section 3.1.

3.3. ABC transporter functionality studies

Investigation of the expression level and functional activity of efflux transporters gives insight into possibilities for reduced bioavailability of nasal drug candidates that are subject to efflux. There is a vast knowledge regarding drug transporters in the gastrointestinal tract, as well as those with a clinically significant function in the hepatic and renal drug clearance. However, the expression of efflux transporters in the human and animal nasal cavity has been elucidated only recently [30]. The identification and characterization of functional transporters in the nasal mucosa can aid the recognition of drug candidates having the adequate properties for nasal administration. It is also important to consider that the contribution of active transport to the drug's permeability is relevant for low and moderate permeability drugs. Higher possibility of incorrect classification of permeability exists for drug substances that undergo efflux in comparison with passively transported drugs, if the extent of efflux transporter expression in the *in vitro* cell model is lower than the expression level in human epithelium, or if there is no expression of a particular efflux transporter in the *in vitro* model [21].

In our RPMI 2650 cell models, in addition to already performed gene expression profiling [11], we investigated the functional activity of two well-known efflux transporters P-gp (ABCB1) and BCRP (ABCG2). Bidirectional transport assays were performed using rhodamine123 and rosuvastatin as substrates for P-gp and BCRP, respectively. Additional bidirectional permeability assessment of the aforementioned efflux substrates was conducted in the presence of verapamil and PSC-833 as first- and second- generation P-gp inhibitors [31] and BCRP inhibitor Ko143.

3.3.1. P-gp functional studies

The measured P_{app} s for rhodamine123 with and without used inhibitor substances are shown in Fig. 2.

The efflux ratio (ER) of rhodamine123 in absence of inhibitors in both A-L and L-L models is far below 2 (ER = 0.8 and 0.9 for the RPMI 2650 A-L and L-L model, respectively). This indicates lack of functional activity of P-gp. The FDA and ICH guidelines on demonstrating method suitability for permeability determination [21,22] advocate the use of bidirectional transport studies of recommended substrates for showing asymmetric permeability and functional expression of the efflux transporters. A compound that is a substrate for efflux transporters exhibits an ER > 2, whose value decreases when appropriate inhibitor is added [21,22]. In our study, the P_{app} of rhodamine123 in the B-A

direction for both RPMI 2650 A-L and L-L models did not significantly change after addition of verapamil and PSC-833 as inhibitors ($p > 0.05$) and the ER of rhodamine123 remained around 1 in all cases (Fig. 2). Namely, for the A-L model, the obtained ER in presence of verapamil and PSC-833 was 1.2 and 0.9, respectively; for the L-L model, the ER = 0.9 and 1.0 when using verapamil and PSC-833, respectively.

Contradictory results for the functional expression of P-gp in the RPMI 2650 cells are published to date [15,19]. Namely, in different experimental settings, Dolberg and Reichl [15] and Mercier et al. [19] confirmed functional expression of P-gp. However, they did not observe P-gp activity when bidirectional transport experiments were done [19]. The addition of the inhibitor verapamil did not decrease the ER of rhodamine123 as expected [19]. This lack of active involvement of P-gp in the efflux of rhodamine123 is in agreement with the results from our bidirectional transport studies. The lack of functional activity of P-gp in both RPMI 2650 cell models can be related to the low level of *ABCB1* expression [11]. The *ABCB1* expression was found to be 32-fold and 400-fold lower for the RPMI 2650 A-L and L-L cell model, respectively, when compared to the Caco-2 cells expression level [11,23]. Dolberg and Reichl [15] published comparable results in terms of P-gp mRNA expression level in A-L and L-L RPMI 2650 models. Mercier et al. [19] also propose the same hypothesis of ABC transporter expression level not being high enough to be reflected as measurable efflux of substrates in bidirectional transport studies.

In contrast, functional activity of P-gp in primary human nasal epithelial cells has been confirmed in a study by Cho et al. [32], using 5 μ M rhodamine123 and having the same experimental set up for the bidirectional transport studies of rhodamine123 as in our current work. Cho et al. [32] have shown strong efflux of rhodamine123 in their study, with the P_{app} of rhodamine123 being 6.9-fold higher in the B-A than in A-B direction.

Since the goal of the *in vitro* nasal cell models is to closely match the barrier properties of human nasal epithelium, it is important to observe analogous expression level of P-gp in human nasal mucosa. The study by Al-Ghabeish et al. [30] reported moderate gene and protein expression of P-gp in the respiratory nasal mucosa of humans. The *ABCB1* was also expressed in excised human nasal tissue [15]. However, the P-gp efflux activity in excised human nasal mucosa could not be demonstrated by using rhodamine123 as a substrate. Instead P-gp functional activity in the *ex-vivo* tissue was confirmed with the substrate [H^3]digoxin [15].

Recently, Mercier et al. [33] investigated the expression and functionality of four ABC transporters in the organotypic airway tissue model MucilAir™, by protein mass spectrometry and bidirectional transport experiments using adequate substrates and inhibitors. A 100-fold lower abundance of the P-gp in MucilAir™ than in Caco-2 cells was reported. The functionality of the P-gp was confirmed by obtaining an ER of 6 for the substrate rhodamine123, which was reduced by approximately 65% in the presence of the inhibitor verapamil [33].

3.3.2. BCRP functional studies

Rosuvastatin is known to be a BCRP substrate, while Ko143 is considered as highly selective inhibitor of this ABC transporter [34]. The P_{app} s obtained for rosuvastatin in absence and presence of Ko143 are shown in Fig. 3A. As evident, the ER of rosuvastatin was close to 1.0 and was not significantly altered when Ko143 was present in the apical donor solution ($p > 0.05$), implying that the BCRP is not functionally active in any of the tested RPMI 2650 cell models. Our previous investigation of the BCRP expression at mRNA level shows that *ABCG2* is moderately expressed in both RPMI 2650 A-L and L-L cell model after 1 and 3 weeks of culturing [11]. Pozzoli et al. [35] published data on BCRP gene expression in the RPMI 2650 A-L cell model which is in good agreement with our data [11]. They also compared the BCRP gene expression in RPMI 2650 A-L cell model with that in primary human nasal cells, reporting that this transporter is expressed in both investigated cell models [35]. Interestingly, very different results

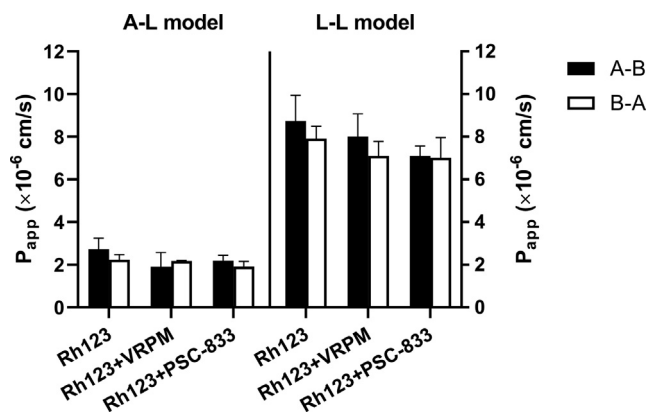


Fig. 2. Apparent permeability coefficients (P_{app} s) of rhodamine123 (Rh123) in absence and presence of the inhibitors verapamil (VRPM) and PSC-833 measured in the A-L (left part of the graph) and L-L (right part of the graph) RPMI 2650 cell model. Data are expressed as the mean \pm SD. SD, standard deviation.

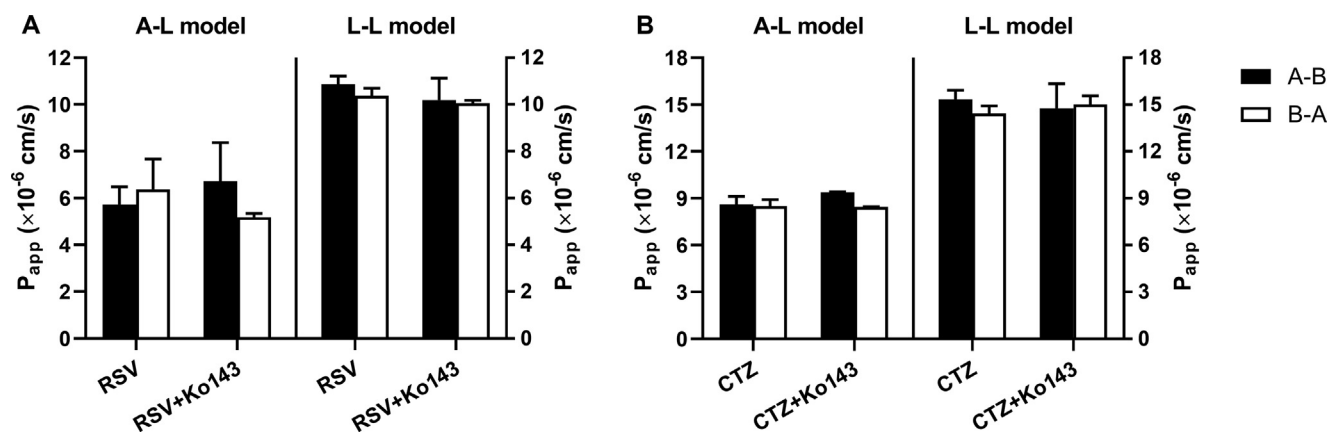


Fig. 3. Apparent permeability coefficients (P_{app} s) of rosvastatin (RSV) (A) and chlorothiazide (CTZ) (B) in absence and presence of the inhibitor Ko143 measured in the A-L and L-L RPMI 2650 cell models. Data are expressed as the mean \pm SD. SD, standard deviation.

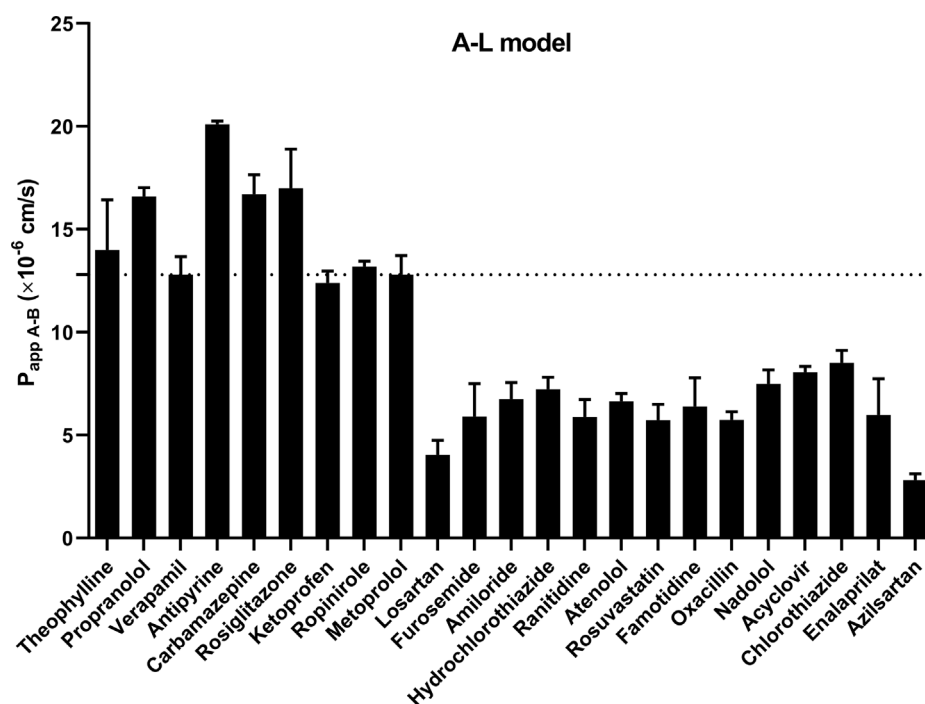


Fig. 4. Apparent permeability coefficients (P_{app} s) for the A-L RPMI 2650 cell model in A-B direction for all tested model drugs. Data are expressed as mean \pm SD ($n \geq 3$). SD, standard deviation. The dotted line represents the P_{app} of metoprolol as a low/high BCS permeability class boundary reference compound.

regarding the expression of *ABCG2* in human and animal nasal mucosa were obtained in a study by Al-Ghabeish et al. [30]. The microarray determination revealed weak gene expression in the human nasal mucosa, while *ABCG2* was highly expressed in the nasal mucosa of the investigated animal species [30]. The expression of *ABCG2* was also demonstrated to be approximately 15-fold lower in both RPMI 2650 cell models [11] compared to expression in the Caco-2 cells, which does not translate well to the protein expression levels later reported by Mercier et al. [19]. Specifically, using cell-based ELISA, they reported higher protein expression of BCRP in the cells of the RPMI 2650 A-L model when compared to the Caco-2 cells [19]. They also carried out intracellular accumulation assays using fluorescent BCRP substrate Hoechst 33342 and Ko143 as inhibitor, which showed functional expression of BCRP at cellular level in the A-L model [19]. On the other hand, their bidirectional transport studies using 50 μ M chlorothiazide as BCRP substrate and Ko143 as specific inhibitor did not show functionally active BCRP at the epithelial level, since the use of the inhibitor did not significantly alter the ER of 1.9 [19], which is very much in

accordance with our results.

By employing chlorothiazide as a BCRP substrate [23,36] in our experiments, the ER value was again close to 1.0 and not significantly different when Ko143 was added ($p > 0.05$), confirming a lack of functional activity of BCRP in both RPMI 2650 cell models (Fig. 3B) at the epithelial level.

3.4. Permeability of drug substances across the RPMI 2650 cell models

We have founded the evaluation of suitability of two RPMI 2650 cell line models for nasal drug permeability determination on the recommendations from ICH's and US-FDA's guidance on demonstrating method suitability of *in vitro* permeability methods [21,22]. The guidelines recommend the use of a minimum of 5 model drugs from each permeability category (low, moderate and high), in order to characterize the full permeability range, with a minimum of 3 replicates to provide a reliable estimate of drug permeability [21,22]. Moreover, at least 20 model drugs encompassing the entire range of absorption

should be included [21,22]. In addition to 5 zero permeability markers, we used 7 drugs with low intestinal absorption (enalaprilat, acyclovir, chlorothiazide, nadolol, oxacillin, famotidine, azilsartan), 7 moderately permeable drugs (ranitidine, amiloride, atenolol, hydrochlorothiazide, furosemide, losartan, rosuvastatin) and 9 highly permeable drugs to evaluate the suitability of the two RPMI 2650 cell models for nasal drug permeability determination.

3.4.1. Permeability of highly permeable drug substances

The tested highly permeable model drugs are transported across the epithelial cells predominantly by passive diffusion (transcellular route). The lowest P_{app} s for this set of drug substances tested in the A-L RPMI 2650 model were determined for metoprolol, ketoprofen, verapamil and ropinirole (Fig. 4). Among these, ropinirole, metoprolol and ketoprofen have the lowest oral absorbed fraction (f_a) (Table 1). Moreover, metoprolol is often used as a high permeability reference standard in intestinal permeability models having permeability in close vicinity to the low/high BCS permeability class boundary [37,38]. Thus, it is viewed as suitable highly permeable compound for aiding classification of drugs in appropriate BCS permeability categories. The P_{app} values of all other tested compounds are either very similar or higher than that of metoprolol and most importantly, they are clearly distinguished from the medium and low permeability model drugs. Like in intestinal permeability models, metoprolol can be used as an internal standard during drug permeability assessment. According to the FDA's or ICH's guidance on permeability assays, metoprolol could be used together with a low [21] or moderate permeability [22] model drug as a second internal standard during drug permeability assessment in order to demonstrate the consistency of the permeability testing method.

In the L-L RPMI 2650 model, metoprolol had the lowest P_{app} value among the tested high permeability model drugs (Fig. 5). None of the tested substances had shown efflux (ER < 2). The measured P_{app} values for the high permeability model drugs in A-B and B-A direction for the A-L and L-L RPMI 2650 models are shown in Table 2 and 3, respectively.

3.4.2. Permeability of moderately and low permeable drug substances

The permeability of 7 model drugs (losartan, furosemide, amiloride,

hydrochlorothiazide, ranitidine, rosuvastatin and atenolol) classified as moderately permeable according to the value of oral absorbed fraction (f_a) was assessed in bidirectional permeability studies. The obtained P_{app} values in the A-B direction for the A-L model are below the P_{app} value of metoprolol and span from 4×10^{-6} cm/s to 7.3×10^{-6} cm/s, with losartan having the lowest measured P_{app} among the moderate permeability model drugs. As can be observed in Fig. 4, the A-L model very reliably distinguishes between the highly permeable drugs and those with moderate and low permeability. The obtained P_{app} values for 7 tested model drugs from the low permeability class (enalaprilat, acyclovir, chlorothiazide, nadolol, oxacillin, famotidine, azilsartan) are also clearly lower than the P_{app} value for metoprolol, while both tested RPMI 2650 nasal epithelial models obviously do not distinguish between the drugs with moderate permeability and those with low permeability designation (Fig. 4 and Fig. 5) in the intestinal absorption *in vivo* and in the relevant intestinal permeability models like Caco-2. With the current lack of *in vivo* nasal absorption data we must concede that it is unclear whether a difference between these two permeability classes for the nasal mucosa even exists *in vivo*.

The P_{app} values of most moderate permeability compounds obtained with the L-L model are not clearly distinguishable from the P_{app} of metoprolol (Fig. 5). This shows that the L-L model is really not suitable for use in the classification of drug permeability. Moreover, it was observed that the L-L RPMI 2650 cell model is leakier compared to its A-L counterpart as shown by the obtained P_{app} values of FDs with different molecular weight, as well as by the lower TEER values compared to the TEER values for the A-L cell model.

The ER for all compounds tested with the A-L and with the L-L RPMI 2650 models not only remained below 2 but were very close to 1.0, indicating a general lack of efflux transporter activity for these two nasal mucosa cell models. It is noteworthy that some of the tested model drugs with moderate permeability (furosemide, losartan, ranitidine and rosuvastatin) and all of those with low permeability except enalaprilat, oxacillin and azilsartan were previously shown to be efflux transporter substrates in the Caco-2 cell model [23,39], where the concentrations of the P-gp substrates used during the bidirectional transport experiments were the same as for the study presented here.

Oxacillin is considered to be a substrate for the PEPT1 (SLC15A1)

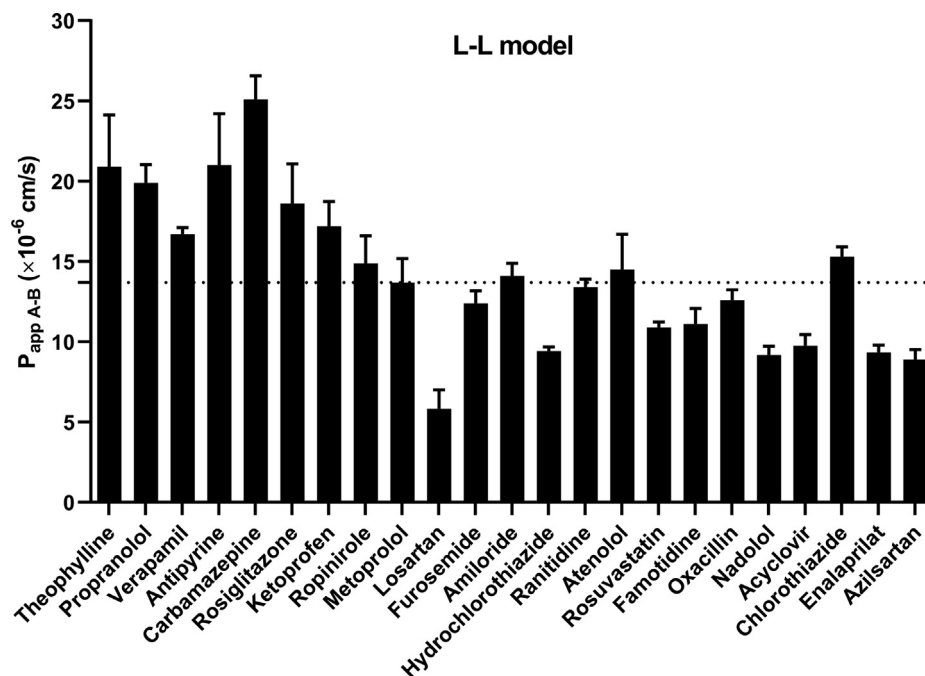


Fig. 5. Apparent permeability coefficients (P_{app} s) for the L-L RPMI 2650 cell model in A-B direction for all tested model drugs. Data are expressed as mean \pm SD ($n \geq 3$). SD, standard deviation. The dotted line represents the P_{app} of metoprolol as a low/high BCS permeability class boundary reference compound.

Table 2Apparent permeability coefficients (P_{app}) and efflux ratio (ER) of 23 tested model drugs with high, moderate and low permeability in the A-L RPMI 2650 cell model.

A-L RPMI 2650 model					
Model drug	$P_{app\ A-B}$ ($\times 10^{-6}$ cm/s)	SD ($\times 10^{-6}$ cm/s)	$P_{app\ B-A}$ ($\times 10^{-6}$ cm/s)	SD ($\times 10^{-6}$ cm/s)	ER
Theophylline	14.0 (n = 4)	2.4	15.4 (n = 3)	1.7	1.1
Propranolol	16.6 (n = 3)	0.4	16.4 (n = 3)	1.9	1.0
Verapamil	12.8 (n = 4)	0.9	13.1 (n = 4)	0.6	1.0
Antipyrine	20.1 (n = 4)	0.2	20.6 (n = 3)	2.0	1.0
Carbamazepine	16.7 (n = 3)	1.0	17.0 (n = 3)	0.4	1.0
Rosiglitazone	17.0 (n = 4)	1.9	20.8 (n = 4)	1.8	1.2
Ketoprofen	12.4 (n = 4)	0.6	13.1 (n = 4)	0.6	1.1
Ropinirole	13.2 (n = 3)	0.3	13.7 (n = 4)	0.6	1.0
Metoprolol	12.8 (n = 5)	0.9	11.8 (n = 7)	1.7	0.9
Losartan	4.1 (n = 6)	0.7	3.4 (n = 7)	0.9	0.8
Furosemide	5.9 (n = 6)	1.6	5.2 (n = 7)	1.1	0.9
Amiloride	6.8 (n = 4)	0.8	5.9 (n = 4)	1.1	0.9
Hydrochlorothiazide	7.2 (n = 5)	0.6	7.3 (n = 7)	1.0	1.0
Ranitidine	5.9 (n = 7)	0.9	5.2 (n = 6)	0.6	0.9
Atenolol	6.6 (n = 3)	0.4	7.0 (n = 3)	0.9	1.1
Rosuvastatin	5.7 (n = 3)	0.8	6.0 (n = 3)	1.3	1.1
Famotidine	6.4 (n = 4)	1.4	6.6 (n = 4)	0.5	1.0
Oxacillin	5.8 (n = 3)	0.5	5.0 (n = 3)	0.3	0.9
Nadolol	7.5 (n = 3)	0.7	6.0 (n = 4)	0.7	0.8
Acyclovir	8.1 (n = 3)	0.3	9.1 (n = 4)	0.4	1.1
Chlorothiazide	8.5 (n = 4)	0.6	4.7 (n = 3)	0.1	0.6
Enalaprilat	6.0 (n = 3)	1.8	7.1 (n = 3)	0.6	1.1
Azilsartan	2.8 (n = 3)	0.3	3.1 (n = 4)	0.2	1.1

transporter [40,41]. In Caco-2 cells where only the PEPT1 is expressed, the obtained ER in a study by Jarc et al. [23] was only 0.3. The expression level of *SLC15A1*, however, is significantly (1000-fold) lower in RPMI 2650 cells grown at both interfaces than in Caco-2 model [11,23]. This is in line with the obtained ER ~ 1 for oxacillin in both RPMI 2650 cell models characterized in the present study. On the other hand, the PEPT1 transporter was found to be expressed and functional in the primary cultured human nasal epithelial cells [9,42].

3.5. Comparison of drug absorption in RPMI 2650 cell models and in MucilAir™, Caco-2 cells and isolated rat jejunum model

A meaningful comparison of drug permeability characteristics can

be made between the RPMI 2650 cell lines and the human nasal mucosa. As already mentioned, the morphological closeness of the *in vitro* cell model to the human nasal mucosa is one of the fundamental traits of a suitable nasal barrier model. It is known that squamous cells are the exclusive cell type constituting the RPMI 2650 cell multilayers [8,13], while the fully differentiated human nasal epithelial model MucilAir™ predominantly consists of columnar ciliated cells [33]. The better differentiation ability of the primary human nasal epithelial cells into goblet and ciliated cells [43,44] enables closer match to the nasal epithelial architecture *in vivo* [45].

We therefore compared the model drug permeability in the two RPMI 2650 cell models to the permeability in the 3D model of human airway epithelium MucilAir™, again showing that the A-L RPMI 2650

Table 3Apparent permeability coefficients (P_{app}) and efflux ratio (ER) of 23 tested model drugs with high, moderate and low permeability in the L-L RPMI 2650 cell model.

L-L RPMI 2650 model					
Model drug	$P_{app\ A-B}$ ($\times 10^{-6}$ cm/s)	SD ($\times 10^{-6}$ cm/s)	$P_{app\ B-A}$ ($\times 10^{-6}$ cm/s)	SD ($\times 10^{-6}$ cm/s)	ER
Theophylline	20.9 (n = 3)	3.2	18.5 (n = 3)	0.5	0.9
Propranolol	19.9 (n = 3)	1.1	19.0 (n = 3)	1.3	1.0
Verapamil	16.7 (n = 4)	0.4	19.0 (n = 4)	0.8	1.1
Antipyrine	21.0 (n = 4)	3.2	21.9 (n = 3)	3.7	1.0
Carbamazepine	25.1 (n = 3)	1.5	23.5 (n = 4)	1.7	0.9
Rosiglitazone	18.6 (n = 4)	2.5	25.0 (n = 4)	1.3	1.3
Ketoprofen	17.2 (n = 3)	1.5	17.7 (n = 4)	0.5	1.0
Ropinirole	14.9 (n = 3)	1.7	15.6 (n = 4)	1.2	1.0
Metoprolol	13.7 (n = 6)	1.5	13.6 (n = 4)	1.6	1.0
Losartan	5.8 (n = 3)	1.2	5.2 (n = 4)	0.4	0.9
Furosemide	12.4 (n = 3)	0.8	10.2 (n = 4)	0.5	0.8
Amiloride	14.1 (n = 4)	0.8	16.0 (n = 4)	0.4	1.1
Hydrochlorothiazide	9.4 (n = 3)	0.3	11.0 (n = 4)	0.5	1.2
Ranitidine	13.4 (n = 3)	0.5	12.4 (n = 4)	0.9	0.9
Atenolol	14.5 (n = 6)	2.2	14.2 (n = 6)	1.8	1.0
Rosuvastatin	10.9 (n = 3)	0.3	10.4 (n = 4)	0.3	1.0
Famotidine	11.1 (n = 4)	1.0	10.7 (n = 6)	1.0	1.0
Oxacillin	12.6 (n = 4)	0.6	11.9 (n = 6)	0.2	1.0
Nadolol	9.2 (n = 3)	0.6	10.9 (n = 4)	1.1	1.2
Acyclovir	9.8 (n = 3)	0.7	10.2 (n = 4)	0.4	1.0
Chlorothiazide	15.3 (n = 4)	0.6	14.4 (n = 4)	0.5	0.9
Enalaprilat	9.3 (n = 3)	0.5	10.6 (n = 3)	0.3	1.1
Azilsartan	8.9 (n = 4)	0.6	7.7 (n = 4)	0.6	0.9

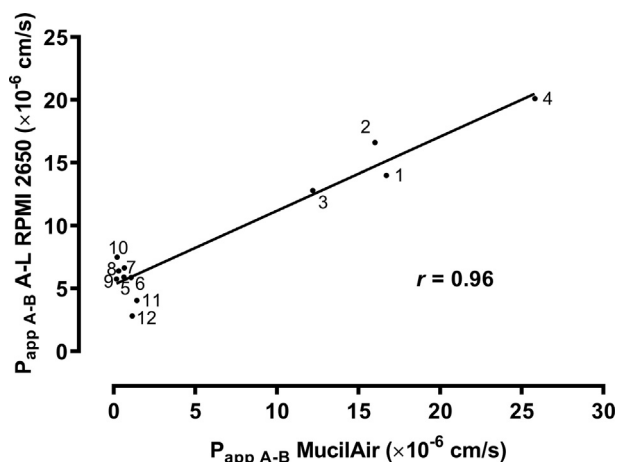


Fig. 6. Correlation between $P_{app} \text{ A-B}$ in A-L RPMI 2650 cell model and $P_{app} \text{ A-B}$ in MucilAir™. P_{app} determined for the following model drugs: 1-theophylline; 2-propranolol; 3- verapamil; 4- antipyrine; 5- furosemide; 6- ranitidine; 7- atenolol; 8- famotidine; 9- oxacillin; 10- nadolol; 11-losartan; 12-azilsartan. r , Pearson correlation coefficient.

cell model is superior to the L-L model for nasal drug permeability studies. The measured P_{app} s in RPMI 2650 cells were correlated with measured P_{app} s in MucilAir™. Some P_{app} s in MucilAir™ were obtained in our laboratory (oxacillin, famotidine, furosemide, losartan, azilsartan), while some were previously published [46]. An excellent correlation has been observed between the permeability values for 12 model drugs determined in RPMI 2650 A-L model and MucilAir™ ($r = 0.96$, $p < 0.0001$) (Fig. 6). The P_{app} s obtained in the 3D model of human airway epithelium range over three orders of magnitude: $1.7 \times 10^{-7} \text{ cm/s}$ (oxacillin) to $2.6 \times 10^{-5} \text{ cm/s}$ (antipyrine). To our knowledge, no efflux in MucilAir™ has been reported for the tested compounds [46]. Similarly, for drugs that were shown to be P-gp substrates in the Caco-2 cell model (losartan, famotidine) [23], we obtained an ER < 2 when testing the permeability of these model drugs in MucilAir™. These results suggest that the P-gp expression in the tested fully differentiated human nasal epithelial model is also insufficient for active efflux of P-gp substrates. Mercier et al. [33] also reported a 100-fold lower expression of the P-gp in MucilAir™ relative to the expression in the Caco-2 cell model. Remarkably, we did obtain an ER of 3.0 for furosemide tested at 1000 μM concentration in MucilAir™. This drug exhibits an ER around 10 in Caco-2 cells at the same concentration [23]. The work of Ebner et al. [47] suggests that BCRP and probably MRP2 are the ABC-transporters involved in the active efflux of furosemide in Caco-2 cells. This, together with the results by Mercier et al. [33] confirming the functional activity of the BCRP in MucilAir™, can explain the ER of 3 for furosemide in our study. The very high linear correlation of the A-L RPMI 2650 results with those obtained with the 3D nasal epithelial model is actually somewhat surprising if we consider the much higher complexity of the later. The mucociliary system can be observed in MucilAir™ [33], while the formation of cilia in the RPMI 2650 model was confirmed not to be present [48]. It is known that the intranasally administered drugs can be cleared from the nose due to the mucociliary clearance, but the effect of limited absorption time obviously cannot be incorporated in *in vitro* determination of the permeability coefficients. It is however as essential for the drug to pass the mucus barrier before crossing the nasal epithelium *in vitro* as it is *in vivo*. Mucus can impede the diffusion of lipophilic drugs and positively charged entities and the mesh space of mucin in the span of 20–200 nm is assumed to represent an obstacle to the diffusion of bigger particles [49]. The RPMI 2650 cells do produce mucoid material on their surface [11] although its composition is not yet characterized [8]. The expression of the secretory mucin MUC5AC in A-L RPMI 2650 cells was shown to be lower than the expression in

porcine olfactory and respiratory primary cells [48]. Nevertheless, the results presented here indicate that mucoid material produced by the RPMI 2650 cells either has a very similar influence on the permeability of the model drugs compared to the mucus of the MucilAir™ or that the overall effect of mucus on drug permeability is not very high. In an analogy to the very common *in vitro* simulation of intestinal permeability with Caco-2 cell line one should also consider that Caco-2 cells do not feature the mucus layer.

Despite the primary nasal cells being morphologically more similar to the *in vivo* nasal mucosa, the RPMI 2650 cells are often considered as a reasonable choice for modeling the nasal epithelia in the early stages of nasal formulation development, due to avoiding variabilities which could be introduced with the use of primary cells [50]. The *in vitro* permeability properties of cell lines modeling the nasal mucosa should be primarily evaluated through the correlation with the *in vivo* fraction of the drug absorbed. However, the only cell line for which a similar feat has been previously achieved was the Caco-2. Since the Caco-2 cell line is used as a model for the intestinal drug absorption, a wealth of reference bioavailability data is available. Another logical step towards the evaluation of suitability of *in vitro* epithelial cell models for nasal drug permeability determination would therefore be to compare the permeability characteristics of the RPMI 2650 cell models with that of Caco-2. Additionally, based on comparably low TEER values of the RPMI 2650 cell line and isolated rat jejunum model, it could be of interest to compare the permeability properties of the RPMI 2650 models with that of isolated rat jejunum and establish the leakiness of RPMI 2650 model relative to the Caco-2 monolayers as an example of a tight barrier. Therefore, the following correlations are additionally presented: (a) a correlation of P_{app} s for all tested model drugs, obtained with the A-L RPMI 2650 cell model and with the Caco-2 model (Fig. 7A) and (b) correlation of P_{app} s from the A-L RPMI 2650 cell model (for all compounds in Table 1, except azilsartan and chlorothiazide) and rat P_{app} s (Fig. 7B). The data on P_{app} s determined in Caco-2 cells and in isolated rat jejunum were gathered from published permeability studies [23,25,51–54].

A good correlation was observed between the P_{app} values obtained in our RPMI 2650 A-L model and the corresponding P_{app} values obtained in Caco-2 cell line ($r = 0.90$, $p < 0.0001$). The P_{app} s determined in the RPMI 2650 A-L model also correlate well with P_{app} s in isolated rat jejunum ($r = 0.89$, $p < 0.0001$). In the later correlation, however, it can be noticed that the range of the P_{app} s in RPMI 2650 A-L cell model and in rat jejunum is confined within roughly two orders of magnitude (10^{-6} cm/s to 10^{-5} cm/s) (Fig. 7B). The differences between the P_{app} s of low or moderately permeable drugs and metoprolol are only 3- to 5-fold in the RPMI A-L cell model and the rat jejunum. For the correlation between the P_{app} s in the RPMI 2650 A-L model and Caco-2 cell line (Fig. 7A) the low and moderately permeable model drugs are all grouped at the beginning of the regression line. With 30- to 60- fold lower Caco-2 P_{app} s than the P_{app} for metoprolol, this group can be easily distinguished from the group of highly permeable drugs while the distinction between the low and moderately permeable drugs is not possible in any of the cell models compared in Fig. 7. There is similar leakiness of the RPMI 2650 cell model and rat jejunum (reported TEER $\sim 80 \Omega\text{cm}^2$ for rat jejunum [55]). On the other hand, the tighter permeability barriers such as Caco-2 cells ($\sim 1000 \Omega\text{cm}^2$) [23] are known to provide higher differences between low and high permeability model drugs.

The established correlation between the P_{app} s in the RPMI 2650 L-L cell model and P_{app} s in the Caco-2 cells for 23 model drugs ($r = 0.79$) again indicates that the L-L cell model is not as suitable as the A-L model for drug permeability assays. Likewise, the correlation between the obtained P_{app} s in the RPMI 2650 L-L model and P_{app} s in rat jejunum supports this notion ($r = 0.81$, $n = 21$).

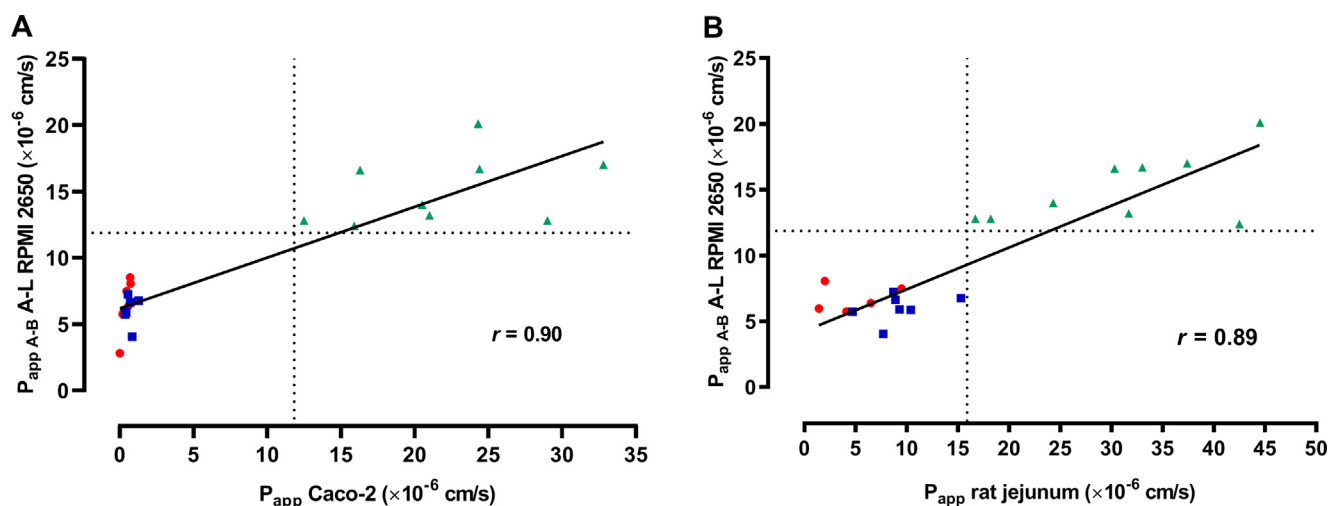


Fig. 7. Correlations between $P_{app\ A-B}$ in A-L RPMI 2650 cell model and P_{app} determined in Caco-2 cells (A) and in isolated rat jejunum (B). Red circles: low permeability model drugs with orally absorbed fraction (f_a) < 50%; blue squares: moderate permeability drugs with $f_a = 50$ –84%; green triangles: high permeability drugs with $f_a \geq 85\%$. The dotted lines represent the P_{app} values for metoprolol as low/high BCS permeability class boundary reference drug.

4. Conclusion

Our study showed that the RPMI 2650 cell line grown at A-L interface is a promising model of the nasal epithelial barrier that could be used in high-throughput permeability assays when screening intranasal candidate drugs and can be appropriate for evaluation of different excipients in formulation development. This model is more suitable than the RPMI 2650 L-L model for drug transport studies, due to superior differentiation between high permeability model drugs and drugs that do not belong to this permeability category. The bidirectional permeability assays using ABC transporter substrates did not reveal functional activity of P-gp and BCRP in any of the investigated RPMI 2650 cell models. Good correlation between the A-L RPMI 2650 cell model and Caco-2 cells was obtained, as well as between the A-L model and isolated rat jejunum. Moreover, excellent correlation was demonstrated between the A-L RPMI 2650 cell model and the 3D human airway epithelia (MucilAir™), substantiating the suitability and relevance of the A-L RPMI 2650 cell layers as a predictive *in vitro* model when assessing intranasal drug permeability.

Declaration of Competing Interest

The authors declared that there is no Conflict of Interest.

Acknowledgements

The authors thank Petra Dujmovič for technical assistance. The authors were supported by Lek Pharmaceuticals, d.d., Sandoz Development Center Slovenia and by Slovenian Research Agency (ARRS) [P1-0189].

Funding sources

This research study did not receive any specific grant from funding agencies in the public, commercial, or not-for-profit sectors.

References

- [1] L. Illum, Nasal drug delivery—possibilities, problems and solutions, *J. Control. Release* 87 (2003) 187–198.
- [2] A. Pires, A. Fortuna, G. Alves, A. Falcao, Intranasal drug delivery: how, why and what for? *J. Pharm. Pharm. Sci.* 12 (2009) 288–311.
- [3] S. Grassin-Delyle, A. Buenestado, E. Naline, C. Faisy, S. Blouquit-Laye, L.J. Couderc, M. Le Guen, M. Fischler, P. Devillier, Intranasal drug delivery: an efficient and non-invasive route for systemic administration: focus on opioids, *Pharmacol. Ther.* 134 (2012) 366–379.
- [4] D.-D. Kim, In Vitro Cellular Models for Nasal Drug Absorption Studies, in: C. Ehrhardt, K.-J. Kim (Eds.), *Drug Absorption Studies: In Situ, In Vitro and In Silico Models*, Springer US, Boston, MA, 2008, pp. 216–234.
- [5] A. Wengst, S. Reichl, RPMI 2650 epithelial model and three-dimensional reconstructed human nasal mucosa as in vitro models for nasal permeation studies, *Eur. J. Pharm. Biopharm.* 74 (2010) 290–297.
- [6] S. Dimova, M.E. Brewster, M. Noppe, M. Jorissen, P. Augustijns, The use of human nasal in vitro cell systems during drug discovery and development, *Toxicol. In Vitro* 19 (2005) 107–122.
- [7] D. Zhang, G. Luo, X. Ding, C. Lu, Preclinical experimental models of drug metabolism and disposition in drug discovery and development, *Acta Pharm. Sin. B* 2 (2012) 549–561.
- [8] C. Mercier, N. Perek, X. Delavenne, Is RPMI 2650 a Suitable In Vitro Nasal Model for Drug Transport Studies? *Eur. J. Drug Metab. Pharmacokinet.* 43 (2018) 13–24.
- [9] A.M. Dolberg, S. Reichl, Expression analysis of human solute carrier (SLC) family transporters in nasal mucosa and RPMI 2650 cells, *Eur. J. Pharm. Sci.* 123 (2018) 277–294.
- [10] J.W. Yoo, Y.S. Kim, S.H. Lee, M.K. Lee, H.J. Roh, B.H. Jhun, C.H. Lee, D.D. Kim, Serially passaged human nasal epithelial cell monolayer for in vitro drug transport studies, *Pharm. Res.* 20 (2003) 1690–1696.
- [11] M.E. Kreft, U.D. Jerman, E. Lasic, T. Lanisnik Rizner, N. Hevir-Kene, L. Peternel, K. Kristan, The characterization of the human nasal epithelial cell line RPMI 2650 under different culture conditions and their optimization for an appropriate in vitro nasal model, *Pharm. Res.* 32 (2015) 665–679.
- [12] G.E. Moore, A.A. Sandberg, Studies of a human tumor cell line with a diploid karyotype, *Cancer* 17 (1964) 170–175.
- [13] P.S. Moorhead, Human tumor cell line with a quasi-diploid karyotype (RPMI 2650), *Exp. Cell Res.* 39 (1965) 190–196.
- [14] S. Bai, T. Yang, T.J. Abbruscato, F. Ahsan, Evaluation of human nasal RPMI 2650 cells grown at an air-liquid interface as a model for nasal drug transport studies, *J. Pharm. Sci.* 97 (2008) 1165–1178.
- [15] A.M. Dolberg, S. Reichl, Expression of P-glycoprotein in excised human nasal mucosa and optimized models of RPMI 2650 cells, *Int. J. Pharm.* 508 (2016) 22–33.
- [16] L. Kurti, S. Veszelka, A. Bocsik, B. Ozsvári, L.G. Puskas, A. Kittel, P. Szabo-Revesz, M.A. Deli, Retinoic acid and hydrocortisone strengthen the barrier function of human RPMI 2650 cells, a model for nasal epithelial permeability, *Cytotechnology* 65 (2013) 395–406.
- [17] S. Reichl, K. Becker, Cultivation of RPMI 2650 cells as an in-vitro model for human transmucosal nasal drug absorption studies: optimization of selected culture conditions, *J. Pharm. Pharmacol.* 64 (2012) 1621–1630.
- [18] A.M. Dolberg, S. Reichl, Activity of multidrug resistance-associated proteins 1–5 (MRP1–5) in the RPMI 2650 cell line and explants of human nasal turbinate, *Mol. Pharm.* 14 (2017) 1577–1590.
- [19] C. Mercier, S. Hodin, Z. He, N. Perek, X. Delavenne, Pharmacological characterization of the RPMI 2650 model as a relevant tool for assessing the permeability of intranasal drugs, *Mol. Pharm.* 15 (2018) 2246–2256.
- [20] C. Bosquillon, M. Madlova, N. Patel, N. Clear, B. Forbes, A Comparison of drug transport in pulmonary absorption models: isolated perfused rat lungs, respiratory epithelial cell lines and primary cell culture, *Pharm. Res.* 34 (2017) 2532–2540.
- [21] FDA U.S. Department of Health and Human Services, Center for Drug Evaluation and Research (CDER), Waiver of In Vivo Bioavailability and Bioequivalence Studies for Immediate-Release Solid Oral Dosage Forms Based on a Biopharmaceutics Classification System. Guidance for Industry, December 2017. <https://www.fda.gov/media/70963/download>, 2017 (accessed 07 January 2019).
- [22] European Medicines Agency, ICH guideline M9 on biopharmaceutics classification system based on biowaivers Step 2b, 2018.

- [23] T. Jarc, M. Novak, N. Hevir, T.L. Rižner, M.E. Kreft, K. Kristan, Demonstrating suitability of the Caco-2 cell model for BCS-based biowaiver according to the recent FDA and ICH harmonised guidelines, *J. Pharm. Pharmacol.* 71 (2019) 1231–1242.
- [24] Center for drug evaluation and research. Application number: 200796Orig1s000 Pharmacology review(s). https://www.accessdata.fda.gov/drugsatfda_docs/nda/2011/200796Orig1s000PharmR.pdf, 2010 (accessed 2 July 2019).
- [25] L. Peternel, K. Kristan, M. Petrussevska, T.L. Rizner, I. Legen, Suitability of isolated rat jejunum model for demonstration of complete absorption in humans for BCS-based biowaiver request, *J. Pharm. Sci.* 101 (2012) 1436–1449.
- [26] P.D. Martin, M.J. Warwick, A.L. Dane, C. Brindley, T. Short, Absolute oral bioavailability of rosuvastatin in healthy white adult male volunteers, *Clin. Ther.* 25 (2003) 2553–2563.
- [27] B. Srinivasan, A.R. Kolli, M.B. Esch, H.E. Abaci, M.L. Shuler, J.J. Hickman, TEER measurement techniques for in vitro barrier model systems, *J. Lab. Autom.* 20 (2015) 107–126.
- [28] H. Kubo, K.-I. Hosoya, H. Natsume, K. Sugibayashi, Y. Morimoto, In vitro permeation of several model drugs across rabbit nasal mucosa, *Int. J. Pharm.* 103 (1994) 27–36.
- [29] D.A. Volpe, Application of method suitability for drug permeability classification, *AAPS J.* 12 (2010) 670–678.
- [30] M. Al-Ghabeish, T. Scheetz, M. Assem, M.D. Donovan, Microarray determination of the expression of drug transporters in humans and animal species used for the investigation of nasal absorption, *Mol. Pharm.* 12 (2015) 2742–2754.
- [31] A. Palmeira, E. Sousa, M.H. Vasconcelos, M.M. Pinto, Three decades of P-gp inhibitors: skimming through several generations and scaffolds, *Curr. Med. Chem.* 19 (2012) 1946–2025.
- [32] H.J. Cho, M.K. Choi, H. Lin, J.S. Kim, S.J. Chung, C.K. Shim, D.D. Kim, Expression and functional activity of P-glycoprotein in passaged primary human nasal epithelial cell monolayers cultured by the air-liquid interface method for nasal drug transport study, *J. Pharm. Pharmacol.* 63 (2011) 385–391.
- [33] C. Mercier, E. Jacquerooux, Z. He, S. Hodin, S. Constant, N. Perek, D. Boudard, X. Delavenne, Pharmacological characterization of the 3D MucilAir nasal model, *Eur. J. Pharm. Biopharm.* 139 (2019) 186–196.
- [34] Q. Mao, J.D. Unadkat, Role of the breast cancer resistance protein (BCRP/ABCG2) in drug transport—an update, *AAPS J.* 17 (2014) 65–82.
- [35] M. Pozzoli, H.X. Ong, L. Morgan, M. Sukkar, D. Traini, P.M. Young, F. Sonvico, Application of RPMI 2650 nasal cell model to a 3D printed apparatus for the testing of drug deposition and permeation of nasal products, *Eur. J. Pharm. Biopharm.* 107 (2016) 223–233.
- [36] E. Beery, Z. Rajnai, T. Abonyi, I. Makai, S. Bansaghi, F. Erdo, I. Sziraki, K. Heredi-Szabo, E. Kis, M. Jani, J. Marki-Zay, G.K. Toth, P. Krajcsi, ABCG2 modulates chlorothiazide permeability—in vitro-characterization of its interactions, *Drug Metab. Pharmacokinet.* 27 (2012) 349–353.
- [37] C.A. Larregieu, L.Z. Benet, Distinguishing between the permeability relationships with absorption and metabolism to improve BCS and BDDCS predictions in early drug discovery, *Mol. Pharm.* 11 (2014) 1335–1344.
- [38] M. Zur, M. Gasparini, O. Wolk, G.L. Amidon, A. Dahan, The low/high BCS permeability class boundary: physicochemical comparison of metoprolol and labetalol, *Mol. Pharm.* 11 (2014) 1707–1714.
- [39] W.J. Hua, H.J. Fang, W.X. Hua, Trans epithelial transport of rosuvastatin and effect of ursolic acid on its transport in Caco-2 monolayers, *Eur. J. Drug Metab. Pharmacokinet.* 37 (2012) 225–231.
- [40] B. Bretschneider, M. Brandsch, R. Neubert, Intestinal transport of beta-lactam antibiotics: analysis of the affinity at the H⁺/peptide symporter (PEPT1), the uptake into Caco-2 cell monolayers and the transepithelial flux, *Pharm. Res.* 16 (1999) 55–61.
- [41] M.E. Ganapathy, M. Brandsch, P.D. Prasad, V. Ganapathy, F.H. Leibach, Differential recognition of beta -lactam antibiotics by intestinal and renal peptide transporters, PEPT 1 and PEPT 2, *J. Biol. Chem.* 270 (1995) 25672–25677.
- [42] R. Agu, E. Cowley, D. Shao, C. Macdonald, D. Kirkpatrick, K. Renton, E. Massoud, Proton-coupled oligopeptide transporter (POT) family expression in human nasal epithelium and their drug transport potential, *Mol. Pharm.* 8 (2011) 664–672.
- [43] H.-J. Cho, U. Termsarasab, J. Kim, D.-D. Kim, In Vitro Nasal Cell Culture Systems for Drug Transport Studies, 2010.
- [44] U. Werner, T. Kissel, In-vitro cell culture models of the nasal epithelium: a comparative histochemical investigation of their suitability for drug transport studies, *Pharm. Res.* 13 (1996) 978–988.
- [45] C. Bitter, K. Suter-Zimmermann, C. Surber, Nasal drug delivery in humans, *Curr. Probl. Dermatol.* 40 (2011) 20–35.
- [46] W. Hoffmann, J. Gradinaru, L. Farcas, M. Caul-Futy, S. Huang, L. Wiszniewski, N. Parissis, S. Morath, S. Fortaner, T. Cole, E. Reginato, P.-A. Carrupt, S. Constant, S. Goecke, Establishment of a human 3D tissue-based assay for upper respiratory tract absorption, *Appl. In Vitro Toxicol.* 4 (2018) 139–148.
- [47] T. Ebner, N. Ishiguro, M.E. Taub, The use of transporter probe drug cocktails for the assessment of transporter-based drug-drug interactions in a clinical setting-proposal of a four component transporter cocktail, *J. Pharm. Sci.* 104 (2015) 3220–3228.
- [48] S. Ladel, P. Schlossbauer, J. Flamm, H. Luksch, B. Mizaikoff, K. Schindowski, Improved in vitro model for intranasal mucosal drug delivery: primary olfactory and respiratory epithelial cells compared with the permanent nasal cell line RPMI 2650, *Pharmaceutics* 11 (2019) 367.
- [49] S. Gänger, K. Schindowski, Tailoring formulations for intranasal nose-to-brain delivery: a review on architecture, physico-chemical characteristics and mucociliary clearance of the nasal olfactory mucosa, *Pharmaceutics* 10 (2018) 11.
- [50] L. Salade, N. Wauthoz, J. Goole, K. Amighi, How to characterize a nasal product. The state of the art of in vitro and ex vivo specific methods, *Int. J. Pharm.* 561 (2019) 47–65.
- [51] D. Dahlgren, C. Roos, P. Johansson, C. Tannergren, A. Lundqvist, P. Langguth, M. Sjoblom, E. Sjogren, H. Lennernas, The effects of three absorption-modifying critical excipients on the in vivo intestinal absorption of six model compounds in rats and dogs, *Int. J. Pharm.* 547 (2018) 158–168.
- [52] I.S. Haslam, D.A. O'Reilly, D.J. Sherlock, A. Kauser, C. Womack, T. Coleman, Pancreatoduodenectomy as a source of human small intestine for Ussing chamber investigations and comparative studies with rat tissue, *Biopharm. Drug Dispos.* 32 (2011) 210–221.
- [53] C. Roos, D. Dahlgren, E. Sjogren, C. Tannergren, B. Abrahamsson, H. Lennernas, Regional intestinal permeability in rats: a comparison of methods, *Mol. Pharm.* 14 (2017) 4252–4261.
- [54] P. Miona, Suitability of Rosuvastatin as a Specific Marker OG ABCG2 Transporter Activity in Mucous Membrane of the Rat Small Intestine, University of Ljubljana, Ljubljana, 2016, p. 58.
- [55] R.M. Menon, W.H. Barr, Comparison of cefitibuten transport across Caco-2 cells and rat jejunum mounted on modified ussing chambers, *Biopharm. Drug Dispos.* 24 (2003) 299–308.